

An improved bio-optical model for the remote sensing of *Trichodesmium* spp. blooms

T. K. Westberry and D. A. Siegel

Institute for Computational Earth System Science, University of California, Santa Barbara, California, USA

A. Subramaniam

Lamont-Doherty Earth Observatory, Columbia University, Palisades, New York, USA

Received 2 June 2004; revised 15 January 2005; accepted 10 March 2005; published 25 June 2005.

[1] The cyanobacterium *Trichodesmium* spp. can be an important ecological and biogeochemical component for both the coastal and open ocean ecosystems by way of its nitrogen fixation ability. However, information regarding its spatial and temporal distribution remains sparse. *Trichodesmium* has unique optical properties that should allow for its spectral signature to be detectable in satellite ocean color data sets. Here, a global data set of concurrent measurements of *Trichodesmium* abundance and radiometric reflectance was compiled and used to develop bio-optical models for *Trichodesmium*. The most robust global model related the water-leaving radiance signal to the identification of an occurrence of a *Trichodesmium* bloom above a threshold value of 3200 trichomes L^{-1} . Using the in situ data set, this model is trained to successfully predict *Trichodesmium* blooms ($\sim 92\%$) while minimizing false positive retrievals ($\sim 16\%$ of nonbloom observations). A validation of the approach applied to Sea-viewing Wide Field-of-view Sensor (SeaWiFS) ocean color imagery shows that the model correctly predicts 76% of the bloom occurrences of an independent validation data set of in situ *Trichodesmium* observations. Ultimately, maps of *Trichodesmium* bloom occurrence will provide a means of addressing the ecology of *Trichodesmium* and its contribution to new production of the world oceans.

Citation: Westberry, T. K., D. A. Siegel, and A. Subramaniam (2005), An improved bio-optical model for the remote sensing of *Trichodesmium* spp. blooms, *J. Geophys. Res.*, 110, C06012, doi:10.1029/2004JC002517.

1. Introduction

[2] Nitrogen fixation in the world oceans has received increasing attention in the recent decade due to revised rate estimates which imply significant contributions to regional and global biogeochemical cycling of carbon and nitrogen [Michaels *et al.*, 1996; Gruber and Sarmiento, 1997; Karl *et al.*, 1997; Capone *et al.*, 1997]. *Trichodesmium*, a colonial, filamentous cyanobacterium, appears responsible for a large portion of this N_2 fixation (although the recognized phylogenetic groups that contribute to global N_2 fixation are becoming more diverse [e.g., Zehr *et al.*, 2001]). Observations of the spatial and temporal distribution of these organisms on regional and global scales are sparse, despite being studied for several decades now. They are universally distributed throughout the tropical and subtropical oceans, yet the transient nature of *Trichodesmium* blooms has made their study difficult. As a result, present quantitative estimates of *Trichodesmium* abundance and its associated N_2 fixation rates still have a large degree of uncertainty in them.

[3] Satellite remote sensing methods provide great potential for making large-scale estimates of *Trichodesmium* abundance on regional to global scales. Previous attempts at developing empirical algorithms for discriminating *Trichodesmium* have worked well on the data they were developed from, but as of yet, no globally applicable bio-optical algorithm relating *Trichodesmium* to satellite remote sensing measurements exists. *Trichodesmium* have unique optical properties that should allow them to be detected from satellite orbit including (1) increased absorption in the near-UV and blue portion of the spectrum due to high amounts of associated colored dissolved organic matter (CDOM) [Steinberg *et al.*, 2004], and water-soluble, UV-absorbing pigments [Subramaniam *et al.*, 1999a], (2) higher relative reflectance near 570 nm due to phycoerythrin fluorescence [Borstad *et al.*, 1992; Subramaniam *et al.*, 1999b], and (3) increased backscatter across all wavelengths caused by the index of refraction change within intracellular gas vacuoles [Borstad *et al.*, 1992; Subramaniam *et al.*, 1999b]. It is thought that each of these features should be manifest in an ocean reflectance spectrum when *Trichodesmium* is present in sufficient quantities, such as that under bloom conditions. Although they generally exist in low background concentrations, episodic blooms of extremely high concentration have been observed ($\sim 10^6$ trichomes

Table 1. Sources of Data for In Situ ($N = 130$) and Satellite Data Set ($N = 142$) and Ranges of *Trichodesmium* Abundance and In Situ Bulk Chl-*a*

Date	Location	<i>Trichodesmium</i> , trichomes L^{-1}	Chl- <i>a</i> , $mg\ m^{-3}$	N^a	Reference
Sept. 1994	Sargasso Sea	0–12	0.06–0.26	13	unpublished
Nov. 1999	Arafura/Timor Sea	146–11,071	0.06–0.82	26 (28)	
April 1998	southwest Pacific	879–6293	0.09–0.11	3 (54)	
Jan. 2001	tropical Atlantic	66–2339	0.01–0.22	14 (8)	Capone <i>et al.</i> [2005]
July 2001	tropical Atlantic	21–73	0.03–0.04	26 (15)	Capone <i>et al.</i> [2005]
Aug. 2003	Sargasso Sea	0–1426	0.00–2.68	26 (26)	unpublished
1995–1999	tropical Atlantic	0–2860	0.11–0.30	22 (11)	Tyrell <i>et al.</i> [2003]

^aNumbers in parentheses are cloud-free observations in satellite data set.

L^{-1} [Devassy *et al.*, 1978; Creagh, 1985; Carpenter and Capone, 1992, and references therein]), albeit never with direct radiometric measurements. A satellite based method for estimating the presence of *Trichodesmium* blooms would provide an ideal way to estimate the biogeochemical impact of these blooms.

[4] Here, we compiled all available concurrent radiometric measurements and equivalent indices of *Trichodesmium* abundance to evaluate past *Trichodesmium*-specific bio-optical models and to develop new methods. As a result, an inverse semianalytic ocean color model, adapted from Garver and Siegel [1997], is used to provide a determination of the *Trichodesmium*-specific chlorophyll concentration, Chl_{tri} . This model is capable of indicating the presence or absence of equivalent *Trichodesmium* biomass above a threshold value (3200 trichomes L^{-1}) with a high degree of fidelity. The model is validated when applied to the Sea-viewing Wide Field-of-view Sensor (SeaWiFS) ocean color data set using independent observations of *Trichodesmium* abundance. Last, an example of application to SeaWiFS ocean color imagery is shown to demonstrate the utility of the model in assessing aspects of the ecology of *Trichodesmium*.

2. Methods

2.1. Field Observations of Reflectance and *Trichodesmium* Abundance

[5] Coincident measurements of ocean optical properties and *Trichodesmium* abundances were compiled from a number of cruises throughout the subtropical oceans from 1994 to present (Table 1). Some were collected as part of large-scale oceanographic programs (e.g., Bermuda Atlantic time series, Atlantic Meridional Transect, NSF Biocomplexity, N_2 fixation, etc.) while others came from individual *Trichodesmium* oriented research expeditions. Each record in this data set contains corresponding estimates of in situ above water, spectral remote sensing reflectance, $R_{rs}(0^+, \lambda)$, *Trichodesmium* abundance, and phytoplankton chlorophyll *a* concentration, chl *a* ($N = 130$). Remote sensing reflectance was calculated for the six SeaWiFS wavebands (412, 443, 490, 510, 555, and 665 nm) as

$$R_{rs}(0^+, \lambda) = \frac{1 - r}{n^2} \frac{L_u(0^-, \lambda)}{E_d(0^-, \lambda)}, \quad (sr^{-1}) \quad (1)$$

where r is the average specular reflectance at the sea surface, $\sim 3\%$ Austin [1974], and n is the index of refraction of seawater, taken as 1.341. $L_u(0^-, \lambda)$ is the spectral

upwelling radiance just beneath the sea surface measured by a profiling spectroradiometer, and $E_d(0^+, \lambda)$ is the incident spectral irradiance above the sea surface measured by a similar radiometer in air. All measurements and calculations adhere to the SeaWiFS ocean optics protocols [Mueller *et al.*, 2002].

[6] *Trichodesmium* collection and enumeration was performed slightly differently among the various cruises. In general, a full Niskin bottle (~ 12 L) of seawater was collected near the surface and gravity filtered through ~ 10 μm mesh. The filter contents were preserved with low-concentration Paraformaldehyde (2–4%) and *Trichodesmium* abundance was determined by epifluorescent microscopy. The other method employed was collection via a plankton net outfitted with a flowmeter (usually 202 μm mesh). The net was deployed for a specified length of time and colonies were picked from the cod end, preserved and counted as above. All values are nominal surface values, but are taken anywhere from 0–5 m depth. For standardization purposes, colony abundances were converted to equivalent trichomes per liter using a value of 200 trichomes col^{-1} [Carpenter, 1983]. In addition, chlorophyll *a* concentrations were determined either fluorometrically or via HPLC pigment analysis and represents bulk phytoplankton chlorophyll. *Trichodesmium*-specific chlorophyll, Chl_{tri} , was estimated from trichome abundance using values of 50 ng chl *a* col^{-1} [Carpenter, 1983].

2.2. Satellite Observations and an Independent Validation Data Set

[7] An independent data set of *Trichodesmium* observations was used to validate the accuracy of our approach when applied to satellite imagery. Reflectance spectra, $R_{rs}(0^+, \lambda)$, were provided from SeaWiFS normalized water-leaving radiance determinations. Spectra were extracted from level 3 GAC data with ~ 9 km resolution at times and locations collocated with the *Trichodesmium* observations. Of the 142 matchups, 77 were satellite overpasses during the shipboard observations described in the previous section. The remaining 65 were additional *Trichodesmium* abundance estimates without in situ radiometry. Together, these data constitute a second independent data set of matched *Trichodesmium*- $R_{rs}(0^+, \lambda)$ suitable for model validation purposes. The satellite determined reflectance spectra were quality controlled by excluding observations where the atmospheric correction may be suspect. In particular, pixels with the aerosol model spectral slope greater than 1.1 (i.e., $\epsilon_{78} > 1.1$) or an aerosol optical thickness spectral slope greater than 0.5 (i.e., $\tilde{A}_{510} > 0.5$)

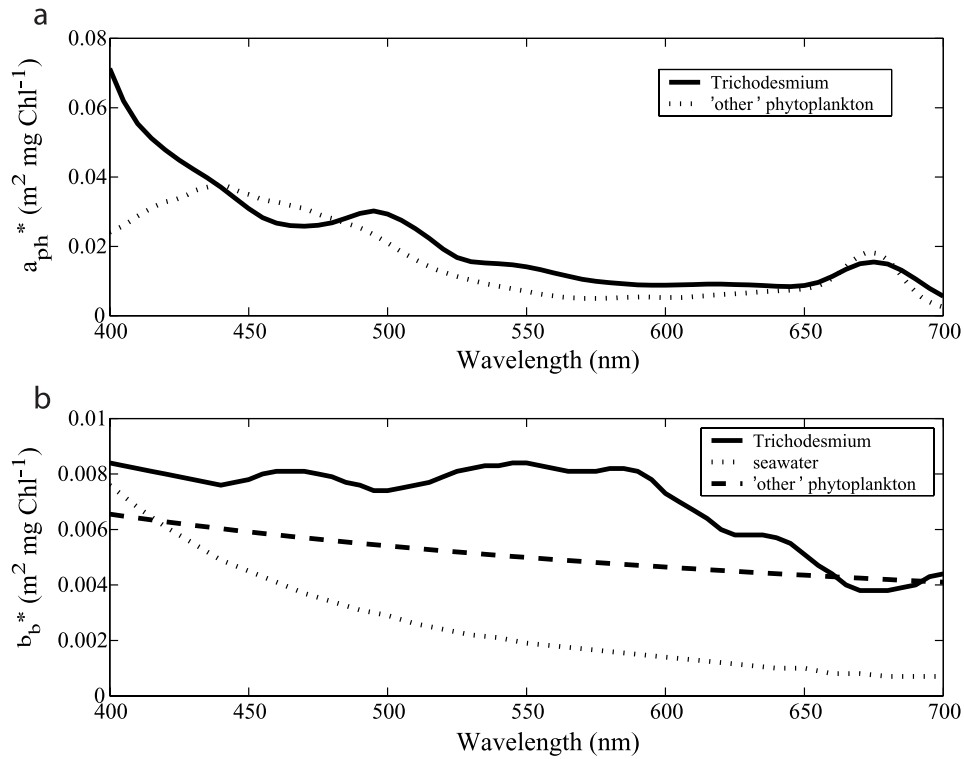


Figure 1. Chlorophyll-specific absorption and backscattering spectra included in the model. (a) *Trichodesmium* (bold line [Subramaniam *et al.*, 1999a]), “other” phytoplankton (dotted line [Bricaud *et al.*, 1998]). (b) *Trichodesmium* (bold line [Subramaniam *et al.*, 1999b]), “other” particulates (dashed line [Morel and Maritorena, 2001]), and water calculated as $0.5 \times$ total water scattering (dotted line [Smith and Baker, 1981]).

were discarded. This screening process eliminated nine additional paired measurements.

2.3. *Trichodesmium*-Specific Reflectance Model

[8] The bio-optical model of Garver and Siegel [1997] and Maritorena *et al.* [2002] was extended to retrieve *Trichodesmium* abundances. In this framework, $R_{rs}(\lambda)$ is related to the absorbing and backscattering properties of the water, or

$$R_{rs}(\lambda) = \sum_{i=1}^2 g_i \left\{ \frac{b_b(\lambda)}{b_b(\lambda) + a(\lambda)} \right\}^i. \quad (2)$$

Absorption, $a(\lambda)$, and backscatter, $b_b(\lambda)$, coefficient spectra can be decomposed into additive components including *Trichodesmium*:

$$a(\lambda) = a_w(\lambda) + a_{ph}(\lambda) + a_{cdm}(\lambda) + a_{tri}(\lambda) \quad (3a)$$

$$b_b(\lambda) = b_{b_w}(\lambda) + b_{b_p}(\lambda) + b_{b_{tri}}(\lambda). \quad (3b)$$

Here, the subscripts w , ph , p , cdm , and tri refer to the absorption and backscattering due to water, phytoplankton, total particulates, colored dissolved and detrital matter, and *Trichodesmium*, respectively. Each component is then

parameterized by a series of known or proscribed spectral shapes and unknown magnitudes:

$$a_{ph}(\lambda) = \text{Chl } a_{ph}^*(\lambda), \quad (4)$$

$$a_{tri}(\lambda) = C_1 \text{Tri } a_{tri}^*(\lambda), \quad (5)$$

$$a_{cdm}(\lambda) = a_{cdm}(\lambda_o) \exp[-S(\lambda - \lambda_o)], \quad (6)$$

$$b_{b_p}(\lambda) = 0.416 \text{Chl}^{0.766} \left[0.002 + 0.02(0.5 - 0.25 \log \text{Chl}) \left(\frac{550}{\lambda} \right) \right], \quad (7)$$

$$b_{b_{tri}}(\lambda) = C_2 \text{Tri } b_{b_{tri}}^*(\lambda), \quad (8)$$

where the unknown quantities are; Chl, the chlorophyll a concentration, Tri, the *Trichodesmium* abundance in trichomes L^{-1} and $a_{cdm}(\lambda_o)$, the absorption by CDM at a scaling wavelength ($\lambda_o = 443 \text{ nm}$). In practice, the *Trichodesmium* abundance is equated to *Trichodesmium*-specific chlorophyll using constant values of $50 \text{ ng chl } a \text{ col}^{-1}$ and $200 \text{ trichomes } \text{L}^{-1}$ [Carpenter, 1983]. Several quantities are specified in the model including the chlorophyll specific phytoplankton absorption spectrum,

Table 2. Parameter Values and Sources Used in Final Model Formulation

Name	Description	Units	Value or Source
a_w	absorption by water	m^{-1}	<i>Pope and Fry</i> [1997]
a_{ph}^*	Chl-specific phytoplankton absorption	$\text{m}^2 \text{mg Chl}^{-1}$	<i>Bricaud et al.</i> [1998]
a_{tri}^*	Chl-specific <i>Trichodesmium</i> absorption	$\text{m}^2 \text{mg Chl}^{-2}$	<i>Subramaniam et al.</i> [1999a]
bb_w	backscattering by water	m^{-1}	<i>Smith and Baker</i> [1981]
bb_p	particulate backscattering	m^{-1}	<i>Morel and Maritorena</i> [2001]
bb_{tri}^*	Chl-specific <i>Trichodesmium</i> backscatter	$\text{m}^2 \text{mg Chl}^{-2}$	<i>Subramaniam et al.</i> [1999b]
S	spectral slope of CDM absorption		<i>Maritorena et al.</i> [2002]
C_1	adjustment for <i>Trichodesmium</i> absorption		0.7097
C_2	adjustment for <i>Trichodesmium</i> backscatter		0.2864

$a_{ph}^*(\lambda)$ (taken from *Bricaud et al.* [1998]) and S , the spectral slope of the CDM absorption curve [*Maritorena et al.*, 2002]. The relationship describing particulate backscatter, $bb_p(\lambda)$ is taken from *Morel and Maritorena* [2001]. *Trichodesmium* chlorophyll-specific absorption and backscattering spectra were taken from *Subramaniam et al.* [1999a, 1999b]. These values are shown spectrally in Figure 1. Upon substitution, equation (2) can be inverted and solved by nonlinear least squares techniques for the three unknown quantities, Chl, Tri and $a_{cdm}(\lambda_o)$. The coefficients, C_1 and C_2 , were added to modify the amplitude of *Trichodesmium* absorption and backscatter to account for potential differences in the bio-optics between laboratory observations of *Subramaniam et al.* [1999a, 1999b] (Table 2) and field populations of *Trichodesmium* as well as for uncertainties in the conversions used to relate *Trichodesmium*-specific chlorophyll concentration, trichome abundance and colony abundance. Optimization of these coefficients is described in a later section.

3. Results and Discussion

3.1. Data

[9] The distribution of *Trichodesmium* abundance in the present data set ranges from 0 to 11000 trichomes L^{-1} , with a mean value of ~ 2100 trichomes L^{-1} (Figure 2a). However, values are not normally distributed about the mean and the median is significantly different (1250 trichomes L^{-1})

suggesting that the infrequent large blooms dominate the statistics of the data set. Over 50% of the observations are less than 100 trichomes L^{-1} and 75% are below 1000 trichomes L^{-1} . The upper range of this data set can be described as a very diffuse to a moderate sized bloom [*Carpenter and Capone*, 1992]. Nonetheless, the maximum values in this data set are much lower than previous estimates made under heavy bloom conditions (e.g., $\sim 10^6$ trichomes L^{-1} [*Devassy et al.*, 1978; *Creagh*, 1985; *Carpenter and Capone*, 1992, and references therein]). The associated in situ determined chl a concentrations are log-normally distributed between 0.01 and 1.3 mg m^{-3} (mean chl $a \sim 0.2 \text{ mg m}^{-3}$ (Figure 2b)). These values are surprisingly low given the amount of *Trichodesmium* biomass present. For example, the highest abundances of *Trichodesmium* in the present data set ($\sim 10^4$ trichomes L^{-1}) should have chlorophyll a concentrations of nearly 3 mg m^{-3} , if average values of 50 ng chl a per colony and 200 trichomes per colony are used [*Carpenter and Romans*, 1991; *Subramaniam et al.*, 1999a, 1999b].

[10] The reflectance spectra associated with the above *Trichodesmium* and chlorophyll a distributions are shown in Figure 2c. There is a large degree of variability, especially at the blue end of the spectrum, but in general, $R_{rs}(0^+, \lambda)$ values are higher at shorter wavelengths ($\lambda < 500 \text{ nm}$) primarily due to the low chlorophyll concentrations present. The upper 10th percentile of the chlorophyll a distribution exhibit slightly “green-shifted” spectra, but are

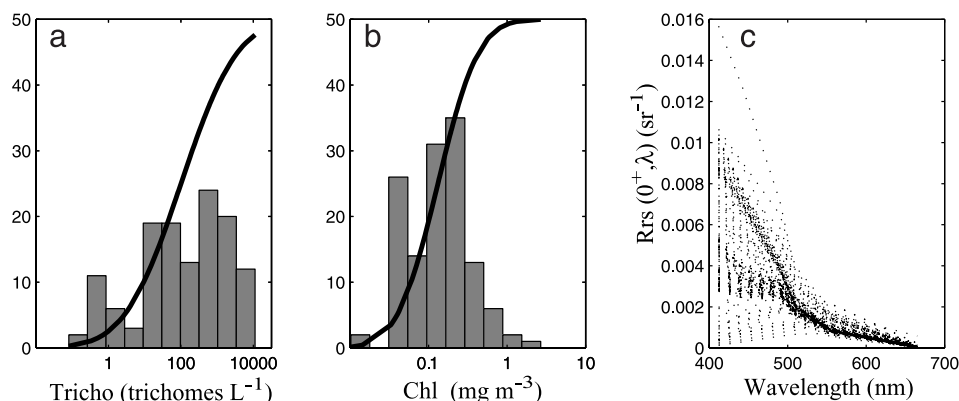


Figure 2. Distribution of observations in the paired *Trichodesmium* and in situ radiometric data set ($N = 130$). (a) *Trichodesmium* abundance (trichomes L^{-1}). (b) Chlorophyll- a concentration ($\text{mg chl } a \text{ m}^{-3}$). (c) Above water, spectral remote sensing reflectance (sr^{-1}). Bold lines in Figures 2a and 2b are cumulative distribution function.

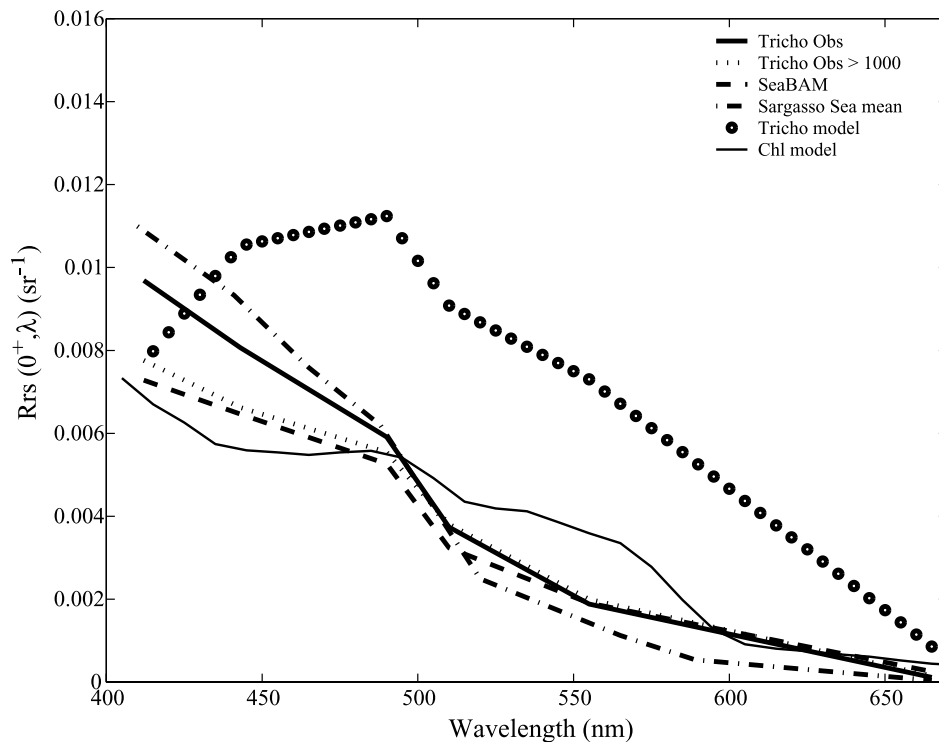


Figure 3. Mean above water spectral remote sensing reflectance for various cases: present in situ observations (bold line), *Trichodesmium* observations >1000 trichomes L^{-1} (dotted line), SeaBAM data (dashed line), Bermuda 1992–1997 (dash-dotted line), *Subramaniam et al.* [2002] model (circles), and non-*Trichodesmium* Case I water model (solid line).

not associated with the higher *Trichodesmium* records ($\langle chl\ a \rangle = 0.55 \pm 0.65\ mg\ m^{-3}$, $\langle Trichodesmium \rangle = 146 \pm 294\ trichomes\ L^{-1}$). Further, many of the hypothesized features of *Trichodesmium* dominated reflectance spectra described in the introduction are not observed.

[11] Figure 3 shows several mean spectra with different optical origins for comparison. Both the mean of the entire data set and the mean of the upper 10th percentile of the *Trichodesmium* distribution are shown and differ only slightly from other spectra. The mean for 6 years of data (1992–1997) collected in the Sargasso Sea is also shown and represents an extreme example of very “blue” or optically clear water. The mean of the SeaBAM data set [O’Reilly *et al.*, 1998] sampled for the same chlorophyll distribution as this data ($0\text{--}1.3\ mg\ m^{-3}$) represents a global average spectrum. The *Trichodesmium* spectra do not appear unlike those of the SeaBAM data set, occupying roughly the same range of $R_{rs}(0^+, \lambda)$ if the chlorophyll distributions are matched. In addition, two model-derived spectra are shown, one containing *Trichodesmium* [Subramaniam *et al.*, 2002] and the other no *Trichodesmium* (Hydrolight 4.1 [Mobley, 1994]), with $Chl_{tri} = 1.0\ mg\ m^{-3}$ and $Chl = 1.0\ mg\ m^{-3}$, respectively. All of the data derived spectra are very similar throughout most of the visible spectrum, diverging near the blue end of the spectrum, and are very different than the two model derived spectra. The $R_{rs}(0^+, \lambda)$ with higher associated *Trichodesmium* abundance (>1000 trichomes L^{-1}) appear slightly less “blue” than the rest of the observa-

tions, but not significantly different (95% confidence) than the mean SeaBAM $R_{rs}(0^+, \lambda)$ at five out of six wavelengths.

3.2. Previous Bio-optical Models for *Trichodesmium*

[12] A handful of empirical bio-optical models describing *Trichodesmium* have been developed during the past decade [Dupouy *et al.*, 1988; Borstad *et al.*, 1992; Subramaniam and Carpenter, 1994; Tassan, 1995; Subramaniam *et al.*, 1999b, 2002]. While each has its merit, only a few of these models can be used to provide a quantitative measure of *Trichodesmium* abundance. Dupouy [1992] described “discolored” waters in the South Pacific as seen in true color CZCS imagery. The discoloration was assumed to be *Trichodesmium* by inference, although there was no ground truth data available. Borstad *et al.* [1992] showed that as the amount of *Trichodesmium* increased, the shape and magnitude of $R_{rs}(\lambda)$ changed, but provided no way of linking the two. Subramaniam and Carpenter [1994] developed a proxy for the presence of *Trichodesmium* in CZCS scenes, but it only provided a relative index of *Trichodesmium* influence on the reflectance from a pixel.

[13] Only Subramaniam *et al.* [2002] presents a quantitative means of estimating the amount of *Trichodesmium* biomass present from a given $R_{rs}(\lambda)$. In this approach a forward remote sensing reflectance model in combination with select SeaWiFS scenes created a set of criteria for screening pixels containing *Trichodesmium* that were

validated against shipboard observations. These criteria tested SeaWiFS, $nL_w(\lambda)$ for certain shape and magnitude characteristics and therefore, allowed the spatial extent of a bloom to be mapped. An empirical relationship then quantified the amount of *Trichodesmium*-specific chlorophyll relative to total chlorophyll as estimated by the operational SeaWiFS algorithm. If we test the $R_{rs}(0^+, \lambda)$ [or equivalent $nL_w(\lambda)$] spectra in the data set presented here, we find that none meet any of the criteria set forth, much less all three simultaneously, as is the requirement to be flagged as *Trichodesmium* (results not shown). This failure is not entirely unexpected as the criteria were partially developed from satellite radiances, unlike the manner of past chlorophyll algorithm building which relies on in situ data [O'Reilly et al., 1998]. The mismatch of scales between in situ measurements and the satellite radiometry was noted by Subramaniam et al. [2002] although no data was available to address this issue. Differences could also be the result of mixed optical assemblages, or the fact that the method of Subramaniam et al. [2002] was developed using only a few SeaWiFS scenes of a single bloom event which might not be representative of the optical variability of *Trichodesmium* in the natural environment.

[14] Although several of the past modeling approaches have shown how $R_{rs}(0^+, \lambda)$ can be influenced by *Trichodesmium*, the diagnosis of a relationship is not always straightforward. It is easily seen how similar the associated $R_{rs}(0^+, \lambda)$ estimates can be to more typical oligotrophic and mesotrophic waters, while still containing “significant” amounts of *Trichodesmium*. Figure 3 very clearly shows that existing bio-optical approaches would not be able to distinguish *Trichodesmium* from moderately elevated “bulk” chlorophyll. It is likely true that at higher abundances, *Trichodesmium* would significantly alter the remote sensing reflectance spectrum and take on the expected spectral shape and magnitude characteristics that have been hypothesized [i.e., Borstad et al., 1992; Subramaniam et al., 2002]. However, while this may be true for large monospecific blooms, mixed phytoplankton assemblages, and thus mixed optical signatures are probably the rule rather than the exception. The modeled spectra of Subramaniam et al. [2002] demonstrate such a case (Figure 3).

[15] The few independent estimates of *Trichodesmium* $R_{rs}(\lambda)$ produced by either model or measurement do show familiar $R_{rs}(\lambda)$ spectra at lower *Trichodesmium* abundance [Borstad et al., 1992; Subramaniam et al., 1999b]. Borstad et al. [1992] showed hypothesized reflectance spectra and in situ measurements of $R_{rs}(\lambda)$ at varying *Trichodesmium* abundances. Measurements made at the lowest concentrations in their dilutions ($\sim 46,000$ trichomes L^{-1}) were 4 times greater than the largest values reported here ($\sim 11,000$ trichomes L^{-1}), yet show only the slightest indication of expected *Trichodesmium* characteristics [see Borstad et al., 1992, Figure 6]. In fact, if the $R_{rs}(\lambda)$ shown by Borstad et al. [1992] were extrapolated to *Trichodesmium* densities similar to those in the data set presented here, they would be in good agreement with measurements presented here (not shown). This can also be seen to a lesser extent in Subramaniam et al. [1999b] which shows very similar $R_{rs}(\lambda)$ between *Trichodesmium*

and other phytoplankton at low to moderate chlorophyll concentrations.

3.3. Application of a Semianalytical Bio-optical Model

[16] Semianalytic ocean color models relate the remote sensing reflectance, $R_{rs}(0^+, \lambda)$, to the inherent optical properties. The model of Maritorena et al. [2002] enables the simultaneous retrieval of the chlorophyll *a* concentration, the absorption coefficient due to colored dissolved and detrital matter (CDM), $a_{cdm}(\lambda_o)$, and particulate backscatter, $b_{bp}(\lambda_o)$, where $\lambda_o = 443$ nm. On the basis of laboratory and field measurements, it seems reasonable that *Trichodesmium* populations will exhibit traits that will enable its remote estimation using this model. Up to 80% of the internal cell volume comprises gas vacuoles [Walsby, 1992; Borstad et al., 1992], resulting in very high backscatter due to the large difference in index of refraction between water, cytoplasm, and the air within the vacuoles. Also, high abundances of *Trichodesmium* leech significant quantities of CDOM, some in the form of microsporine-like amino acids [Steinberg et al., 2004; Subramaniam et al., 1999a]. These properties should act to increase both $b_{bp}(443)$ and $a_{cdm}(443)$.

[17] Application of this model to the in situ data set enables the analysis of these properties as a function of *Trichodesmium* abundance as well as a comparison to a nominal “reference” state, calculated as the mean for the SeaBAM data set over the same chlorophyll range as the in situ data set (Figure 4). The SeaBAM data set likely contains few, if any, *Trichodesmium* observations and represents a globally representative (nonpolar) data set. Mean values for $a_{cdm}(443)$ and $b_{bp}(443)$ are 0.018 and 0.0018 m^{-1} , respectively. While retrieved values of $a_{cdm}(443)$ and $b_{bp}(443)$ are at times 4–10 times higher than the SeaBAM mean values, they are not necessarily associated with high *Trichodesmium* observations. The same is true for determinations of $a_{cdm}(443)$ and $b_{bp}(443)$ per unit chlorophyll (m^2 mg chl a^{-1}). In short, there is no obvious pattern in any of these quantities, precluding their use as predictors of *Trichodesmium* biomass.

3.4. *Trichodesmium*-Specific Model Tuning

[18] The initial *Trichodesmium* bio-optical model (presented in section 2.3) hindcast skill is very poor ($r^2 = 0.08$, RMSE = 0.70, bias > 10^4). This is not surprising, as the model coefficients have been optimized using a mostly non-*Trichodesmium* data set [see Maritorena et al., 2002]. Consequently, a heuristic iterative approach [Press et al., 1990] was applied to determine optimal values for many or all of the parameters, and constitutes a simple “tuning” of the model. In this scheme, a cost function was defined and values of model parameters were drawn from a bounded random normal distribution, applied in the model, and the cost function evaluated (approach follows Maritorena et al. [2002]). Those parameter sets resulting in local minima of the cost function were considered as “optimized coefficients.” The form of the cost function chosen reflects the qualities of the model which were to be emphasized. It initially included standard metrics such as r^2 , RMS error, and normalized mean bias between observed and modeled abundance of *Trichodesmium* trichomes. Free parameters to be optimized included C_1 , C_2 , and S . Each of the candidate

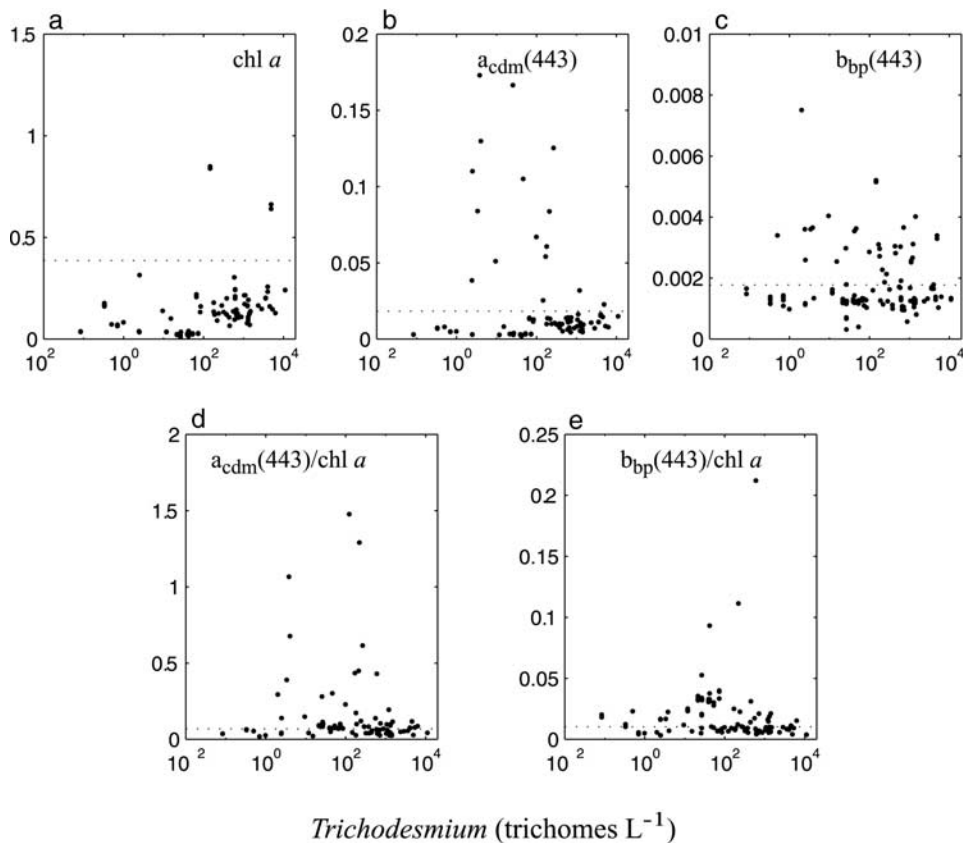


Figure 4. Optical property retrievals using the model of *Maritorena et al.* [2002] for the paired *Trichodesmium* and radiometric observations ($N = 130$): (a) Chl a (mg m^{-3}); (b) $a_{\text{cdm}}(443)$ (m^{-1}); (c) $b_{\text{bp}}(443)$ (m^{-1}); (d) $a_{\text{cdm}}^*(443)$ ($\text{m}^2 \text{mg chl}^{-1}$); and (e) $b_{\text{bp}}^*(443)$ ($\text{m}^2 \text{mg chl}^{-1}$). Horizontal dotted lines represent mean retrieved values for the SeaBAM data set (from *O'Reilly et al.* [1998]).

models were tuned as described above. The number of iterations was dependent on the number of free parameters and ranged from 5×10^4 to 1.6×10^5 and spanned a factor of 3 (300% variability) in each respective parameter space. Although there was improvement in model success upon tuning, a viable 1:1 relationship was not realized ($r^2 < 0.3$ in all cases).

[19] The failure to capture a significant amount of variability in *Trichodesmium* abundance led to a reconsideration of goals and to the assessment of where and when *Trichodesmium* blooms occur and not their level. This casts the cost function in terms of correct and incorrect model estimates (false positive) above some “bloom” threshold, also called “commissions” and “omissions” by *Brown and Yoder* [1994]:

$$\text{CF} = \left(1 - \frac{\#\text{correct bloom}}{\#\text{bloom observations}}\right) + \frac{\#\text{incorrect nonbloom}}{\#\text{nonbloom observations}}.$$

Hence there are only two levels which can be confidently appointed, “bloom” or “nonbloom”. In turn, the identification threshold was determined by a compromise between the values of the two terms in the cost function, the number of omissions and commissions. As the identification

threshold increases, the percentage of false positive retrievals decreases, yet the number of correct bloom predictions also decreases (Figure 5). That is, as we define a bloom at higher *Trichodesmium* abundance, there is obviously more margin for error at subbloom values (i.e., less false positives). However, we also have less and less bloom observations to tune the model with. A bloom value of 3200 trichomes L^{-1} was chosen and represents a reasonable benchmark for bloom conditions. The best candidate model required optimization of only C_1 and C_2 resulting in values of 0.7097 and 0.2864, respectively. Figure 6 shows observed *Trichodesmium* abundance versus modeled abundance using the optimized C_1 and C_2 with a bloom threshold of 3200 trichomes L^{-1} . The model correctly identifies $\sim 92\%$ of “bloom” observations and $\sim 84\%$ of “nonbloom” observations, or $\sim 16\%$ false positive retrievals in the in situ data set.

[20] An independently derived data set of satellite $R_{rs}(0^+, \lambda)$ from SeaWiFS (section 2.2) and collocated *Trichodesmium* observations were used to validate the model. Applying the model correctly identifies 76% of bloom observations and 71% of nonbloom observations (Figure 6). While this is not as good as the in situ results, most of the bloom values are correctly classified. The number of false positive retrievals is larger than expected (29%), but some of these could be excluded using differ-

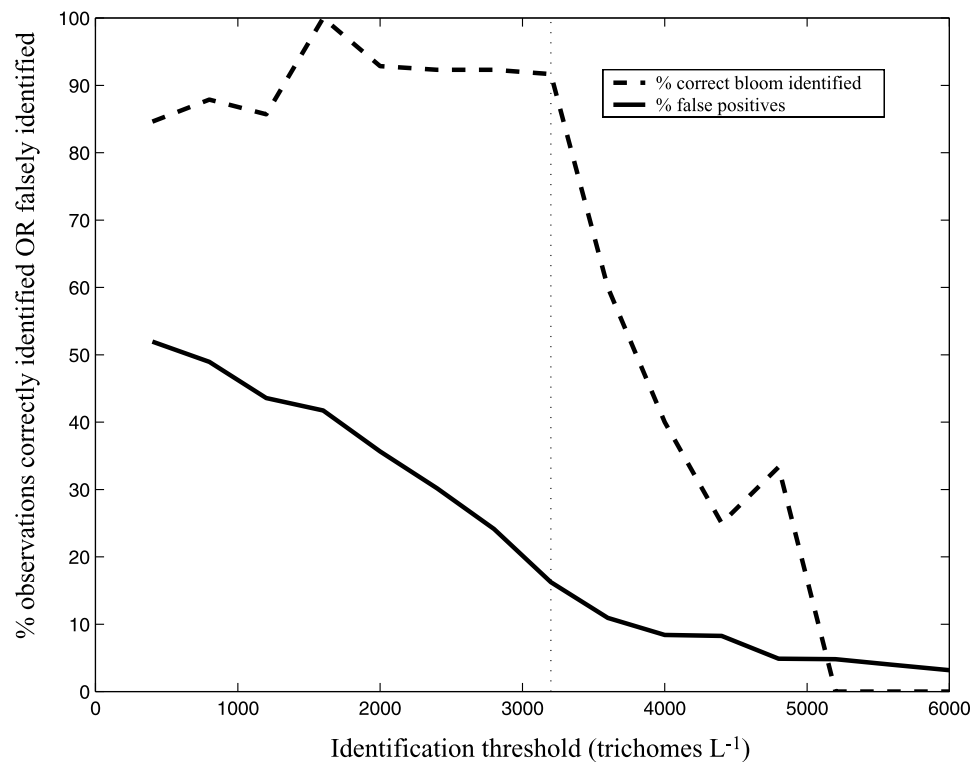


Figure 5. Terms of cost function (CF) as a function of *Trichodesmium* identification threshold. Plotted are % correct bloom retrievals (dashed line) and % false positives (solid line) versus *Trichodesmium* abundance (trichomes L⁻¹). Can also be thought of as (1 - % omissions) and % commissions, respectively.

ent filters. A filter for suspect atmospheric correction was already applied to these data (as described in section 2.2) and flags a handful ($N = 9$) of the false positive retrievals. While this process improves the model statistics in this data set only slightly, a preliminary analysis of SeaWiFS images processed with the model described here show that this procedure successfully eliminates 5–10% of all bloom retrievals. In addition, it appears that some fraction of the false positives occur as isolated pixels with no other positive bloom retrievals in the immediate vicinity (not shown). These too, could be eliminated by applying a morphological erosion filter [e.g., *Brown and Yoder, 1994*]. Lastly, discrimination based on ecological indicators may also be possible. *Trichodesmium* blooms are known to occur in warm surface waters ($>25\text{C}$) and generally under low-wind conditions. By setting thresholds in these and other quantities (PAR, water depth, etc.) pixels could be masked before application of the model. This could effectively limit the number of potential false positive retrievals even further.

[21] The failure to yield absolute *Trichodesmium* abundance estimates is unfortunate as this would allow better resolution in much of the ocean which undoubtedly falls below bloom conditions. Nonetheless, it is instructive to explore the cause of the model's inability to achieve such a relationship. While it may be sufficiently easy to distinguish large discolored patches of water from the surroundings [e.g., *Dupouy, 1992*], natural variability in individual bloom characteristics prevents a scalable relationship to

predict the precise amount of *Trichodesmium*. Some of these characteristics have been noted and are related to age and health of the bloom. Changes in pigmentation of the community accompany the evolution of a bloom and the effects are not well understood. *Borstad et al. [1992]* summarize bloom reports in different growth stages and in different regions of the world as gray, reddish brown, greenish yellow, pale brown, and milk colored. This is a much wider range of optical variability than most phytoplankton taxonomic groups. In addition to the color of a bloom, vertical position in the water column will change the surface reflectance. Though high-light-adapted and buoyant, *Trichodesmium* is found throughout the euphotic zone, and small vertical changes in position can greatly alter satellite visibility. This becomes important as the water-leaving radiance signal is a depth-integrated measurement. *Clayton [2001]* used a numerical model to describe the relationship between bloom intensity and depth and the reflectance at the surface. The author found that *Trichodesmium* near the surface would only be detected in a reflectance signal if concentrations were greater than $1.5 \text{ mg chl } a \text{ m}^{-3}$ (~ 6000 trichomes L⁻¹). Further, this detectability decreases rapidly with depth and becomes invisible at the surface even under extreme bloom conditions at 20 m depth. Using criteria similar to *Subramaniam et al. [2002]* it was also shown that only 25% of observations collected on a cruise in the North Atlantic were detectable even though biomass was relatively high [*Hood et al., 2001*].

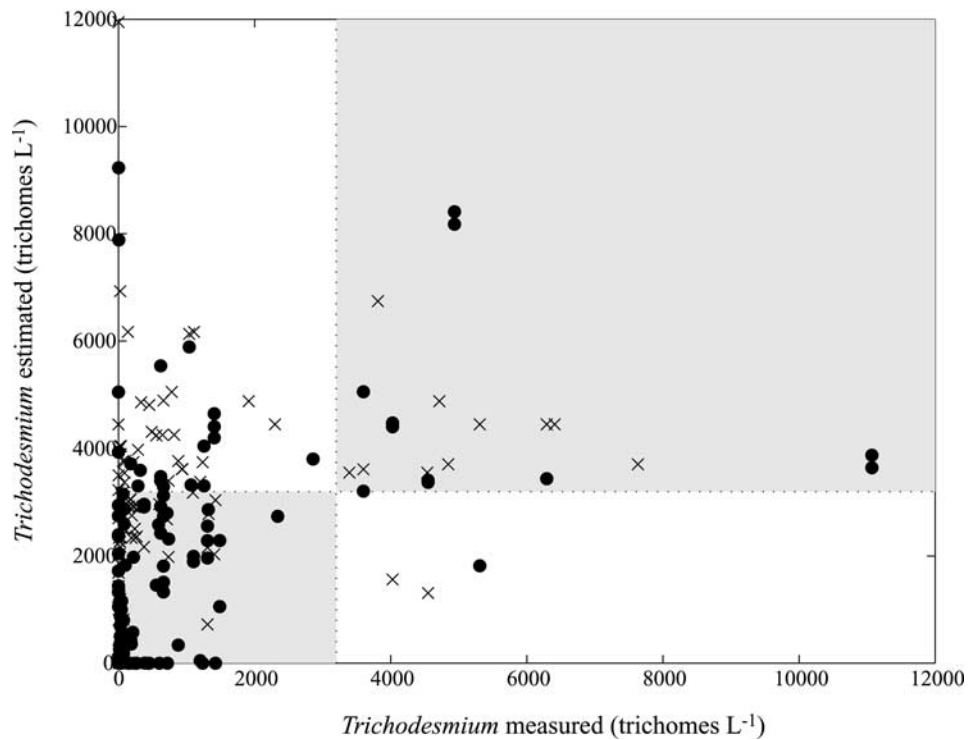


Figure 6. Model estimates of *Trichodesmium* versus observed values (in units of trichomes L^{-1}). Correct prediction horizons are bounded by shaded boxes. Two data sets are shown. Circles are in situ data used to develop the model (i.e., hindcasts); 92% of bloom values are correctly identified, and 16% of nonbloom are observations incorrectly identified ($N = 130$). Crosses are model predictions from Sea Wide Field-of-view Sensor (SeaWiFS)-derived reflectances; 76% of bloom values correctly identified, and 29% of nonbloom observations are incorrectly identified ($N = 133$).

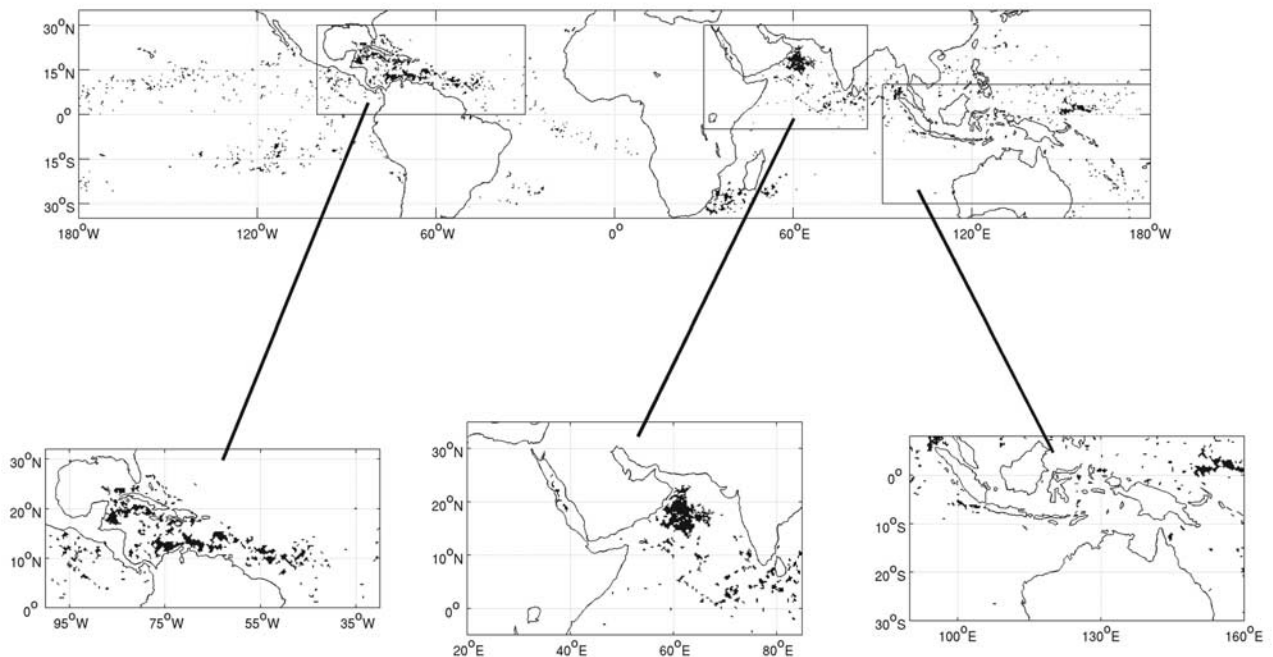


Figure 7. Positive *Trichodesmium* bloom retrievals using SeaWiFS imagery for a single 8 day composite (10–17 February 1998, 0.25° resolution). Shown are a (sub)-tropical view ($35^\circ N$ – $35^\circ S$) and three regional extracts highlighting areas of activity: Gulf of Mexico/Caribbean, Indian Ocean/Arabian Sea, and the western Pacific/Indonesia.

[22] Other sources of uncertainty in the model could stem from variability in the amount of chl *a* per colony and the number of trichomes per colony. Both are well documented and undoubtedly alter the remote sensing reflectance spectrum for a given *Trichodesmium* abundance. The degree of colony self-shading will also affect $R_{rs}(0^+, \lambda)$. This will be a function of bloom density and morphology, themselves a function of bloom age. There are a number of physiological and ecological factors that cumulatively make the model best as a binary indicator of the presence or absence of *Trichodesmium* blooms rather than an algorithm for the accurate determination of its biomass.

3.5. Application to Ocean Color Imagery

[23] A single SeaWiFS 8 day composite (10–17 February 1998, 0.25° resolution) was chosen to demonstrate the utility of the proposed model. Normalized water-leaving radiances were extracted from the image after undergoing standard SeaWiFS processing. These were converted to $R_{rs}(0^-, \lambda)$ and applied to the model, along with the atmospheric screening described above. Results are shown in Figure 7 and include a near-global view (30°N–30°S) and three enlarged subregions. The scale is rather large, and it is difficult to see individual or small groups of pixels (a larger image can be viewed on the web along with other examples at <http://www.icess.ucsb.edu/~toby/tmp/Figure7.png>). However, a very cursory examination of the image reveals a few interesting observations. Very few pixels give positive retrievals, in this image only 1.3% or 6700 out of 518,400 are above the identification threshold (3200 trichomes L^{-1}). In contrast the method of *Subramaniam et al.* [2002] only detects 218 *Trichodesmium* pixels, and 122 of the same pixels. Second, clusters of positive bloom retrievals are not consistent with large-scale oceanographic features, such as those seen in chlorophyll images. Open ocean areas do not seem to have large organized blooms, but likely support subbloom concentrations of *Trichodesmium* (if any). The three zoom maps highlight the areas of greatest retrievals in this image; the Gulf of Mexico and Caribbean, the Arabian Sea, and broad areas of the western Pacific in and around many of the archipelagos there. Some of these areas have observed blooms reported in the literature [*Devassy et al.*, 1978; *Carpenter and Romans*, 1991, and references therein]. The average SeaWiFS chlorophyll in the *Trichodesmium* bloom pixels is 0.23 $mg\ m^{-3}$, compared to a mean of 0.12 $mg\ m^{-3}$ for all noncloudy, nonbloom pixels. However, issues of self-shading within colonies become relevant and must be accounted for [*Borstad et al.*, 1992; *Subramaniam et al.*, 1999b]. Detailed analysis of the spatial and temporal patterns seen in this image and their relation to coincident environmental factors are beyond the scope of this paper, and this single image represents only a brief snapshot of the transient bloom field.

[24] In any event, the sparse nature of the retrievals will make interpretation of maps such as this one difficult. In addition, the space and timescales of the satellite radiances might not match those of *Trichodesmium* bloom dynamics. A multiscale (both space and time) approach will be required to sufficiently characterize the extent of blooms. Additional parameters describing the physical environment at the global scale will be needed as well (i.e., sea surface

temperature, wind speed, mixed layer depth, irradiance, etc.). These and other problems will have to be addressed in order to fully exploit the usefulness of the model.

[25] **Acknowledgments.** The authors would like to acknowledge support from NASA and NSF in the form of an Earth System Science Fellowship (Toby Westberry) and the NSF-funded Biocomplexity-Nitrogen Fixation program, respectively. We would also like to thank two anonymous reviewers and an editorial review that greatly improved the manuscript. Thanks to Doug Capone, Ed Carpenter, Norm Nelson, Debbie Steinberg, Toby Tyrell, and Karen Orcutt for contributing data.

References

- Austin, R. W. (1974), The remote sensing of spectral radiance from below the ocean surface, in *Optical Aspects of Oceanography*, edited by N. G. Jerlov and E. Steemann Nielsen, pp. 317–344, Elsevier, New York.
- Borstad, G. A., J. F. A. Gower, and E. J. Carpenter (1992), Development of algorithms for remote sensing of *Trichodesmium* blooms, in *Marine Pelagic Cyanobacteria: Trichodesmium and Other Diazotrophs*, edited by E. J. Carpenter and D. G. Capone, pp. 193–210, Springer, New York.
- Bricaud, A., A. Morel, M. Babin, K. Allali, and H. Claustre (1998), Variations of light absorption by suspended particles with chlorophyll *a* concentration in oceanic (case 1) waters: Analysis and implications for bio-optical models, *J. Geophys. Res.*, *103*, 31,033–31,044.
- Brown, C. W., and J. A. Yoder (1994), Coccolithophorid blooms in the global ocean, *J. Geophys. Res.*, *99*, 7467–7482.
- Capone, D. G., J. Zehr, H. Paerl, B. Bergman, and E. J. Carpenter (1997), *Trichodesmium*: A globally significant marine cyanobacterium, *Science*, *276*, 1221–1229.
- Capone, D. G., J. A. Burns, J. P. Montoya, A. Subramaniam, C. Mahaffey, T. Gunderson, A. F. Michaels, and E. J. Carpenter (2005), Nitrogen fixation by *Trichodesmium* spp.: An important source of new nitrogen to the tropical and subtropical North Atlantic Ocean, *Global Biogeochem. Cycles*, *19*, GB2024, doi:10.1029/2004GB002331.
- Carpenter, E. J. (1983), Nitrogen fixation by marine *Oscillatoria* (*Trichodesmium*) in the world's oceans, in *Nitrogen in the Marine Environment*, edited by E. J. Carpenter and D. G. Capone, pp. 65–103, Elsevier, New York.
- Carpenter, E. J., and D. G. Capone (1992), Significance of *Trichodesmium* blooms in the marine nitrogen cycle, in *Marine Pelagic Cyanobacteria: Trichodesmium and Other Diazotrophs*, edited by E. J. Carpenter, D. G. Capone, and J. Rueter, pp. 211–217, Springer, New York.
- Carpenter, E. J., and K. Romans (1991), Major role of the cyanobacterium *Trichodesmium* in nutrient cycling in the North Atlantic Ocean, *Science*, *254*, 1356–1358.
- Clayton, T. D. (2001), *Trichodesmium* spp.: Numerical studies of resource competition, carbohydrate ballasting, and remote-sensing reflectance, Ph.D. dissertation, 241 pp., Old Dominion Univ., Norfolk, Va.
- Creagh, S. (1985), Review of literature concerning blue-green algae of the genus *Trichodesmium*, *Bull. 197*, 33 pp., Dept. of Conserv. and Environ., Perth, Australia.
- Devassy, V. P., P. M. A. Bhattathiri, and S. Z. Qasim (1978), *Trichodesmium* phenomenon, *Ind. J. Mar. Sci.*, *7*, 168–186.
- Dupouy, C. (1992), Discoloured waters in the Melanesian archipelago (New Caledonia and Vanuatu): The value of the Nimbis-7 Coastal Zone Colour Scanner observations, in *Marine Pelagic Cyanobacteria: Trichodesmium and Other Diazotrophs*, edited by E. J. Carpenter, D. G. Capone, and J. Rueter, pp. 177–191, Springer, New York.
- Dupuoy, C., Y. Dandonneau, and M. Petit (1988), Satellite detected cyanobacteria bloom in the southwestern tropical Pacific, *Int. J. Remote Sens.*, *8*, 389–396.
- Garver, S. A., and D. A. Siegel (1997), Inherent optical property inversion of ocean color spectra and its biogeochemical interpretation: 1. Time series from the Sargasso Sea, *J. Geophys. Res.*, *102*, 18,607–18,625.
- Gruber, N., and J. L. Sarmiento (1997), Global patterns of marine fixation and denitrification, *Global Biogeochem. Cycles*, *11*, 235–266.
- Hood, R. R., N. R. Bates, D. G. Capone, and D. B. Olson (2001), Modeling the effect of nitrogen fixation on carbon and nitrogen fluxes at BATS, *Deep Sea Res., Part II*, *48*, 1609–1648.
- Karl, D. M., R. Letelier, L. Tupas, J. Dore, J. Christian, and D. Hebel (1997), The role of nitrogen fixation in biogeochemical cycling in the subtropical North Pacific Ocean, *Nature*, *388*, 533–538.
- Maritorena, S., D. A. Siegel, and A. R. Peterson (2002), Optimization of a semianalytical ocean color model for global-scale applications, *Appl. Opt.*, *41*, 2705–2714.
- Michaels, A. F., D. Olson, J. L. Sarmiento, J. W. Ammerman, K. Fanning, A. H. Knap, F. Lipschultz, and J. M. Prospero (1996), Inputs, losses and transformations of nitrogen and phosphorous in the pelagic North Atlantic Ocean, *Biogeochemistry*, *35*, 181–226.

- Mobley, C. D. (1994), *Light and Water: Radiative Transfer in Natural Waters*, Elsevier, New York.
- Morel, A., and S. Maritorena (2001), Bio-optical properties of oceanic waters: A reappraisal, *J. Geophys. Res.*, *106*, 7163–7180.
- Mueller, J. L., et al. (2002), Ocean optics protocols for satellite ocean color sensor validation, revision 3, *NASA Tech. Memo.*, *210004*, 308 pp.
- O'Reilly, J. E., S. Maritorena, B. G. Mitchell, D. A. Siegel, K. L. Carder, S. A. Garver, M. Kahru, and C. McClain (1998), Ocean color chlorophyll algorithms for SeaWiFS, *J. Geophys. Res.*, *103*, 24,937–24,953.
- Pope, R. M., and E. S. Fry (1997), Absorption spectrum (300–700 nm) of pure water: II integrating cavity measurements, *Appl. Opt.*, *36*, 8710–8723.
- Press, W. H., S. A. Teukolsky, W. T. Vetterling, and B. P. Flannery (1990), *Numerical Recipes in C: The Art of Scientific Computing*, Cambridge Univ. Press, New York.
- Smith, R. C., and K. Baker (1981), Optical properties of the clearest natural waters, *Appl. Opt.*, *20*, 177–184.
- Steinberg, D. K., N. B. Nelson, C. A. Carlson, and A. C. Prusak (2004), Production of chromophoric dissolved organic matter (CDOM) in the open ocean by zooplankton and the colonial cyanobacterium *Trichodesmium* spp., *Mar. Ecol. Prog. Ser.*, *267*, 45–56.
- Subramaniam, A., and E. J. Carpenter (1994), An empirically derived protocol for the detection of blooms of the marine cyanobacterium *Trichodesmium* using CZCS imagery, *Int. J. Remote Sens.*, *15*, 1559–1569.
- Subramaniam, A., E. J. Carpenter, D. Karentz, and P. G. Falkowski (1999a), Bio-optical properties of the marine diazotrophic cyanobacteria *Trichodesmium* spp.: I Absorption and photosynthetic action spectra, *Limnol. Oceanogr.*, *44*, 608–617.
- Subramaniam, A., E. J. Carpenter, and P. G. Falkowski (1999b), Bio-optical properties of the marine diazotrophic cyanobacteria *Trichodesmium* spp.: II. A reflectance model for remote sensing, *Limnol. Oceanogr.*, *44*, 618–627.
- Subramaniam, A., C. W. Brown, R. R. Hood, E. J. Carpenter, and D. G. Capone (2002), Detecting *Trichodesmium* blooms in SeaWiFS imagery, *Deep Sea Res., Part II*, *49*, 107–121.
- Tassan, S. (1995), SeaWiFS potential for remote sensing of marine *Trichodesmium* at sub-bloom concentrations, *Int. J. Remote Sens.*, *16*, 3619–3627.
- Tyrell, T., E. Marañón, A. J. Poulton, A. R. Bowie, D. S. Harbour, and E. M. S. Woodward (2003), Large-scale latitudinal distribution of *Trichodesmium* spp. in the Atlantic Ocean, *J. Plankton Res.*, *25*, 405–416.
- Walsby, A. E. (1992), The gas vesicles and buoyancy of *Trichodesmium*, in *Marine Pelagic Cyanobacteria: Trichodesmium and Other Diazotrophs*, edited by E. J. Carpenter, D. G. Capone, and J. Rueter, pp. 141–162, Kluwer Acad., Norwell, Mass.
- Zehr, J. P., J. B. Waterbury, P. J. Turner, J. P. Montoya, E. Omoregie, G. F. Steward, A. Hansen, and D. M. Karl (2001), Unicellular cyanobacteria fix N₂ in the subtropical North Pacific Ocean, *Nature*, *412*, 635–638.

D. A. Siegel and T. K. Westberry, Institute for Computational Earth System Science, University of California, Santa Barbara, CA 93106-3060, USA. (davey@icess.ucsb.edu; toby@icess.ucsb.edu)

A. Subramaniam, Lamont-Doherty Earth Observatory, Columbia University, Palisades, NY 10964-1000, USA. (ajit@ldeo.columbia.edu)